Unclassified

SECURITY CLASSIFICATION OF THIS PAGE

REPORT DOCUMENTATION PAGE

Form Approved
OMB No. 0704-0188
Exp. Date: Jun 30, 1986

1a. REPORT SECURITY CLASSIFICATION Unclassified	1b. RESTRICTIVE MARKINGS
2a. SECURITY CLASSIFICATION AUTHORITY	3. DISTRIBUTION/AVAILABILITY OF REPORT
2b. DECLASSIFICATION/DOWNGRADING SCHEDULE	
4. PERFORMING ORGANIZATION REPORT NUMBER(S) BRL-TR-2847	5. MONITORING ORGANIZATION REPORT NUMBER(S)
6a. NAME OF PERFORMING ORGANIZATION US Army Ballistic Rsch Lab 6b. OFFICE SYMBOL (If applicable) SLCBR-IB	7a. NAME OF MONITORING ORGANIZATION
6c. ADDRESS (City, State, and ZIP Code) Aberdeen Proving Ground, MD 21005-5066	7b. ADDRESS (City, State, and ZIP Code)
8a. NAME OF FUNDING/SPONSORING ORGANIZATION 8b. OFFICE SYMBOL (If applicable)	9. PROCUREMENT INSTRUMENT IDENTIFICATION NUMBER
8c. ADDRESS (City, State, and ZIP Code)	10. SOURCE OF FUNDING NUMBERS PROGRAM ELEMENT NO. 1L263637D155 / PROJECT NO. / TASK NO. / WORK UNIT ACCESSION NO.

11. TITLE (Include Security Classification)

(U) Comparison of Predicted Muzzle Flash for Solid and Regenerative Liquid Propellant Guns

12. PERSONAL AUTHOR(S)

Baer, Paul G., May, Ingo W., and Morrison, Walter F.

13a. TYPE OF REPORT	13b. TIME COVERED	14. DATE OF REPORT (Year, Month, Day)	15. PAGE COUNT
TR	FROM ______ TO ______		

16. SUPPLEMENTARY NOTATION

17. COSATI CODES			18. SUBJECT TERMS (Continue on reverse if necessary and identify by block number)
FIELD	GROUP	SUB-GROUP	Muzzle Flash; Liquid Propellants; Solid Propellants; Solid Propellant Guns; Liquid Propellant Guns

19. ABSTRACT (Continue on reverse if necessary and identify by block number)

Muzzle flash and the associated blast can be a significant problem from the standpoints of both the charge designer and the user on the battlefield. Computer models which describe the muzzle flow of a gun in sufficient detail to provide good predictions of muzzle flash probability have been developed and applied to the case of solid propellant guns. Now these models have been applied to the case of the regenerative liquid propellant gun (RLPG) in order to compare the predicted potential for muzzle flash with that of a conventional solid propellant gun. In the case of the conventional guns, the solid propellant is fuel rich such that the muzzle exhaust gases generally contain a high percentage (30-60%) of combustible species. The fuel rich exhaust gases are mixed with air in the muzzle flow region, shock heated and, if the gas temperature is sufficiently high, ignited, producing "flash" and the associated secondary blast. Muzzle flash calculations for the 155-mm solid propellant gun using M30A1 propellant predict a

20. DISTRIBUTION/AVAILABILITY OF ABSTRACT ☒ UNCLASSIFIED/UNLIMITED ☒ SAME AS RPT. ☐ DTIC USERS	21. ABSTRACT SECURITY CLASSIFICATION
22a. NAME OF RESPONSIBLE INDIVIDUAL Paul G. Baer	22b. TELEPHONE (Include Area Code) 301-278-6187 22c. OFFICE SYMBOL SLCBR-IB-B

DD FORM 1473, 84 MAR — 83 APR edition may be used until exhausted. All other editions are obsolete.

SECURITY CLASSIFICATION OF THIS PAGE

19. ABSTRACT (Con't)

temperature increase of 1187 K in the turbulent afterburning region of the muzzle plume, thus indicating a strong tendency to flash. Calculations for a 155-mm regenerative liquid propellant gun (RLPG) using a stoichiometric, hydroxyl ammonium nitrate (HAN) based liquid propellant, LGP 1845, predict a temperature increase of only 94 K, indicating no tendency to flash. However, calculations using an non-stoichiometric, HAN-based liquid propellant formulation predicted a temperature rise of 633 K, which indicates some tendency to flash.

AD A187174

TECHNICAL REPORT BRL-TR-2847

COMPARISON OF PREDICTED MUZZLE FLASH FOR SOLID AND REGENERATIVE LIQUID PROPELLANT GUNS

PAUL G. BAER
INGO W. MAY
WALTER F. MORRISON

AUGUST 1987

US ARMY BALLISTIC RESEARCH LABORATORY
ABERDEEN PROVING GROUND, MARYLAND

DESTRUCTION NOTICE

Destroy this report when it is no longer needed. DO NOT return it to the originator.

Additional copies of this report may be obtained from the National Technical Information Service, U.S. Department of Commerce, Springfield, VA 22161.

The findings of this report are not to be construed as an official Department of the Army position, unless so designated by other authorized documents.

The use of trade names or manufacturers' names in this report does not constitute indorsement of any commercial product.

TABLE OF CONTENTS

LIST OF FIGURES

LIST OF TABLES

I. INTRODUCTION

The occurrence of muzzle flash in gun systems has long been viewed as an often unavoidable, though undesirable, consequence of the gun and propellant charge design process. While effective chemical and mechanical muzzle flash suppressants have been developed on a largely empirical basis, it was not until Carfagno's[1] classic summary that muzzle flash phenomenology was explained on a scientific basis. Carfagno's methodology was later modified and successfully applied by May and Einstein[2] and Schmidt.[3] With the development of higher performance gun systems and the emergence of a more sophisticated and demanding user, the need to eliminate muzzle flash has become an important factor in propelling charge design. Muzzle flash is undesirable because of increased gun signature, loss of crew night vision and severe blast overpressures associated with the combustion of fuel-rich gun exhaust products outside the gun. It is this combustion process, initiated by the shock heating of the fuel-rich exhaust products entrained with air, that is the source of the important muzzle flash contribution. Phenomenological details of the muzzle flash region have been previously described by Klingenberg[4] and Schmidt.[5]

The dominant factors which determine whether a gun is likely to flash have been summarized by Carfagno.[1] The muzzle exit temperature, pressure, and velocity of the exhaust gases as well as the concentration of the combustibles determine whether flash is likely to occur. These are driven by the adiabatic propellant flame temperature and the thermodynamic efficiency of the particular gun system. The concentration of hydrogen and carbon monoxide, the main fuel ingredients in the exhaust stream, affect the ignition limits for the mixture of air and muzzle gases. For most solid propellant gun systems, the concentration of combustibles ranges from 30 to 70%. Over this range the ignition limits are only weakly affected.

Equilibrium thermodynamic calculations for typical hydroxyl ammonium nitrate-based liquid propellants have shown that the residual combustibles concentrations are on the order of 0.1%. Based on ignition limits presented by Carfagno,[1] which are based on shock tube kinetic data, such low concentrations are unlikely to result in ignition, hence muzzle flash is not likely to occur for liquid propellant guns using basically stoichiometric, oxygen-balanced propellants.

Based on these observations and conclusions it was decided to apply the latest muzzle flash prediction methodology developed over the past few years by Yousefian,[6] in which many of the chemical kinetic details have been worked out by Heimerl.[7] The methodology described in more detail below, couples the output of an interior ballistic code with an equilibrium thermodynamic calculation providing the input conditions for an axisymmetric, quasi-steady flow analysis with detailed chemical kinetics. A temperature rise in the downstream flow represents ignition of the turbulently-entrained fuel air mixture resulting in muzzle flash. The results and conclusions of the application of this more recent muzzle flash prediction technique are discussed below.

II. DESCRIPTION OF MUZZLE FLOW REGION

A brief description of the flow field ahead of the gun muzzle after projectile exit is given here. Details have been previously described.[4 5 8] A simplified schematic of the flow field is illustrated in Figure 1. The main features are a weak precursor blast wave resulting from the air ahead of the projectile and compressed by it. This blast wave has little if any effect on muzzle flash and is consequently ignored in the modeling of it. The three important regions are the transient in-bore evacuation region which determines the crucial input conditions to the next region, the expansion flow field. The expansion region is typical of a highly underexpanded jet with expansion ratios on the order of 500 for most gun situations. The last region of importance is the turbulent region in which afterburning eventually occurs if thermodynamic and chemical kinetic conditions are satisfied.

In the muzzle flash prediction analysis by Yousefian[6] the exit conditions are evaluated by an interior ballistic model[9] coupled with a bore evacuation phase described by Corner[10] and a thermodynamic equilibrium program.[11] These analyses yield transient muzzle pressures, temperatures, gas velocities and chemical species required for input to the expansion region. This procedure has recently been systematized and automated by Keller.[12]

An essential feature of the analysis is that the expansion region depends only on the instantaneous muzzle conditions as shown experimentally by Schmidt and Shear.[5] During the initial expansion process after projectile exit the normal shock (Mach disc) continuously moves away from muzzle leaving behind a lateral shock structure which is largely invariant once established. The behaviour of the Mach disc is considered to be critical in the development of muzzle flash since the heating of the propellant gases strongly influence the occurrence of secondary combustion. At early times almost all of the exhausting gases are processed through the Mach disc. At later times when the exhaust plume has reached its full extent, the Mach disc attains its greatest strength but only processes about 10% of the exhaust flow. The mixing of the exhaust gases which pass through the normal and reflected shocks is assumed to occur instantaneously at the entrance to the turbulent afterburning region. Equilibrium chemistry is assumed for gases passing through the normal shock, while frozen chemistry is assumed for gases passing through the reflected shock. The composition and thermodynamic properties of exhaust gases entering the turbulent afterburning region are averages based on the portion of the flow passing through each of the shocks. This procedure leads to uniform properties for the flow entering the turbulent afterburning region.

For the turbulent afterburning region the steady state eddy diffusivity model by Mikatarian et al.[13] was adapted by Yousefian.[8] While a steady state flow model cannot correctly describe the time dependent behavior of the afterburning flow field, it should result in a flow field which is more likely to burn than a decaying transient flow. Although there are many possible sources for ignition including burning powder particles or other residue, hot gas leakage around the projectile, ignition is considered to be largely the result of the elevated temperature in the gases produced behind the Mach disc.

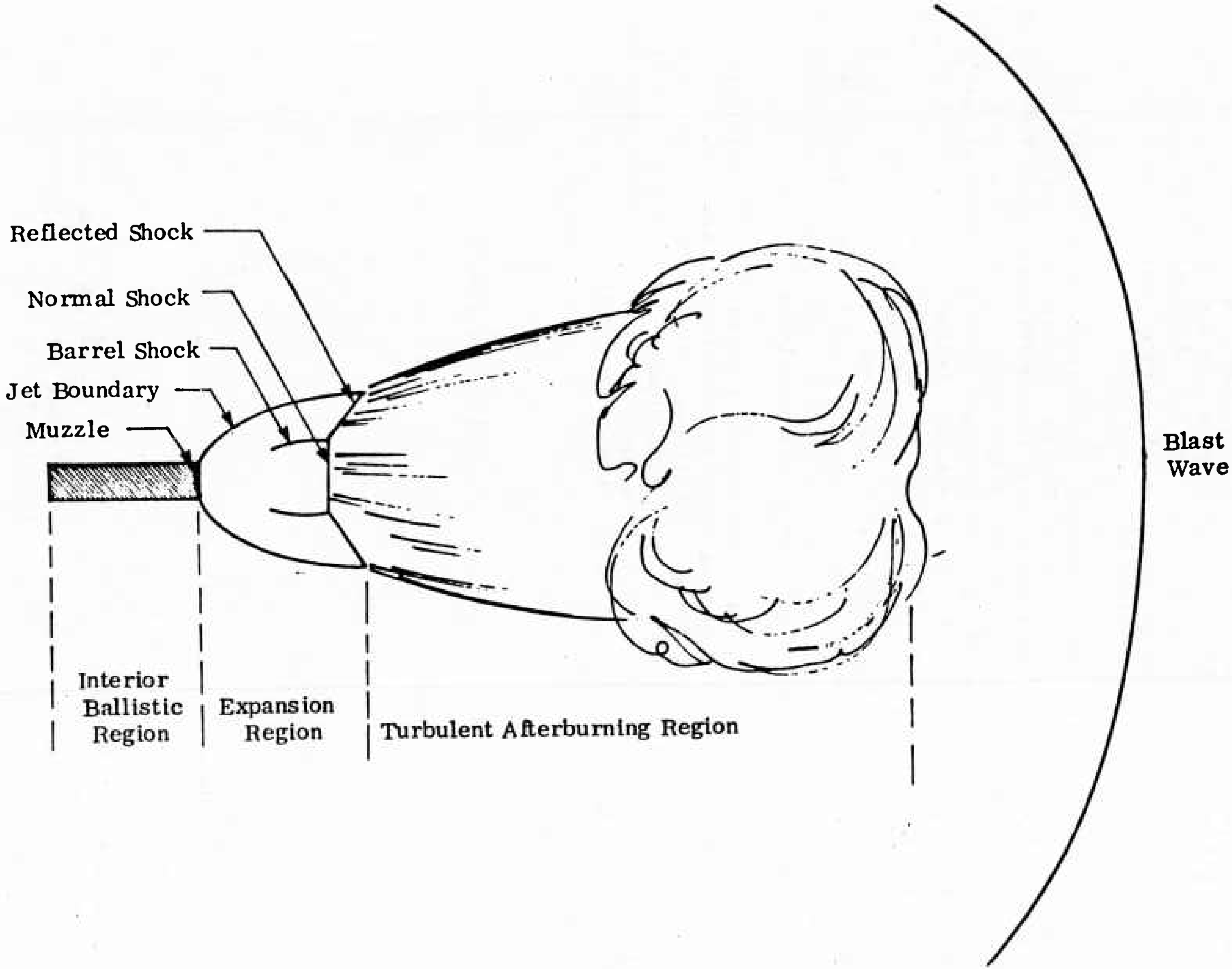

Figure 1. Gun Muzzle Flow Field

III. COMPARISON OF SOLID AND REGENERATIVE LIQUID PROPELLANT GUNS

The muzzle flash properties of solid propellant and liquid propellant guns are compared in this study. Solid propellants are currently used in all fielded guns. As noted previously, these guns are subject to secondary muzzle flash under certain conditions. The use of liquid propellants (LPs) in guns is a relatively recent concept. At present, only experimental fixtures have been fired using an LP.

A schematic of the chamber section of a typical, large caliber solid propellant gun is shown in Figure 2. The gun consists of a thick-walled, cylindrical chamber and tube, and a heavy breech element to seal the rear of the chamber. The projectile and propellant, which is typically contained in a cloth bag for large caliber artillery weapons such as the 155-mm howitzer, are loaded through the breech. The projectile is inserted into the tube and rammed forward until the obturator around the projectile forms a seal with the tube walls. The propelling charge consists of an igniter pad, the solid propellant charge, and small ammounts of additives such as flash suppressants, wear reducing compounds and de-coppering agents. The igniter pad consists of a small quantity of fine grain black powder which is packaged in a cloth bag and attached to the base of the propelling charge.

The composition of the solid propellant is primarily nitrocellulose (single base), nitrocellulose plus nitroglycerin (double base), or nitrocellulose plus nitroglycerin plus nitroguanidine (triple base). The propellant is produced either as cylidrical grains or long tubular sticks which are packaged in a cloth bag. The composition of a typical triple base solid propellant, M30A1, is given in Table 1. All solid gun propellant formulations are fuel-rich.

TABLE 1. M30A1 Solid Propellant Composition

Name	Weight Percent
Nitrocellulose (12.6% N)	27.90
Nitroglycerin	22.42
Nitroguanidine	46.84
Ethyl Centralite	1.49
Potassium Sulfate	1.00
Ethyl Alcohol	0.25
Graphite	0.10

The interior ballistic process is initiated by firing an elecrical or percussion primer through a spit hole in the gun breech. The primer produces hot gas and hot particles which impact the igniter pad attached to the base of the propellaing charge, igniting the rapid burning black

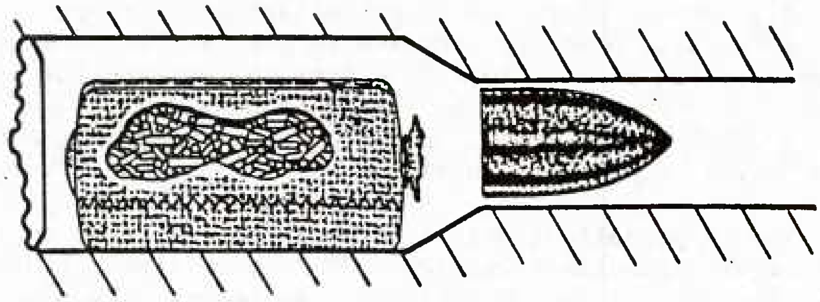

Figure 2. Typical Solid Propellant Gun

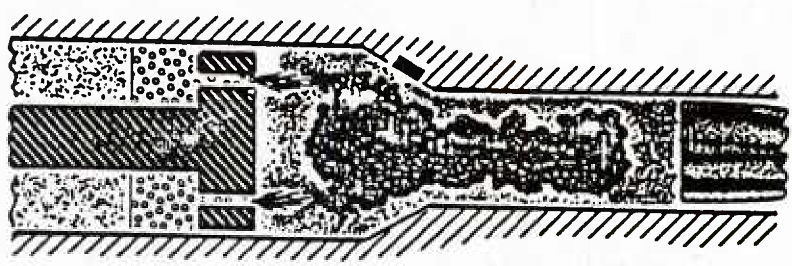

Figure 3. Regenerative Liquid Propellant Gun

powder. As the igniter burns, the hot gas which is produced fills the combustion chamber and begins to permeate into the main solid propellant charge. Eventually the solid propellant ignites and begins to evolve gas rapidly, rupturing the confining cloth bag. When the chamber pressures exceeds the shot start pressure of the projectile, it begins to accelerate down the tube. During the early portion of the process, the gas generation rate of the burning propellant is high enough to produce a rapidly rising pressure despite the system expansion due to projectile motion. The chamber pressure eventually reaches a maximum and then begins to decrease as the rate of gas expansion behind the accelerating projectile exceeds the rate of gas generation. Burnout of the solid propellant prior to projectile exit results in a more rapid pressure decrease as the gas continues to expand. Following the ejection of the projectile from the muzzle, the combustion gases are expelled from the gun, the so-called blow-down phase. The muzzle flow region is described in detail in the previous section. A more detailed discussion of solid propellant gun technology is given in reference 14.

Current liquid propellant gun research is concentrated on the regenerative liquid propellant gun (RLPG)[15 16] utilizing a hydroxyl ammonium nitrate (HAN) based liquid monopropellant. As before, the gun consists of a thick-walled, cylindrical tube and chamber. However, a differential area, regenerative piston has been introduced into the chamber, see Figure 3. The projectile is inserted into the tube as before, and the LP is pumped into the propellant reservoir behind the regenerative piston. The injection orifices in the piston are initially sealed to prevent leakage of propellant into the combustion chamber. Initial pressurization of the combustion is provided by an igniter using either a fine grained solid or a liquid propellant.

The HAN-based liquid propellants are a homogeneous mixture of hydroxyl ammonium nitrate, water, and an organic ammonium nitrate. HAN is itself an oxidizer-rich monopropellant. It is combined with a fuel-rich, organic ammonium nitrate to produce a stoichiometric mixture, ie. the equilibrium products of combustion are CO_2, H_2O, and N_2. The amount of water in the propellant is then adjusted to fix the total nitrate concentration at 11 molar. The composition of a typical HAN-based liquid propellant, LGP 1845, is provided in Table 2.

TABLE 2. HAN 1845 Liquid Propellant Composition

Name	Weight Percent
Hydroxyl Ammonium Nitrate	63.23
Triethanolammonium Nitrate	19.96
Water	16.81

The RLPG interior ballistic cycle is initiated by firing an electrical or percussion primer into the igniter charge, which burns, producing hot, high pressure gases in the combustion chamber. As the chamber pressure increases, the regenerative piston is pushed to the rear, pressurizing the liquid propellant in the reservoir. Since the area of the chamber face of the piston is larger than that of the reservoir face, the liquid reservoir pressure will be higher than the chamber pressure during normal operation. The increasing reservoir pressure will eventually rupture the orifice seals, initiating propellant injection. The liquid propellant enters the combustion chamber as a jet, which will breakup into a fine spray and burn rapidly. When the chamber pressure exceeds the shot start pressure of the projectile, it begins to accelerate down the tube. As in the case of the solid propellant gun, the gas generation rate during the early portion of the cycle dominates the gas expansion, producing a rapidly increasing chamber preesure. The pressure will reach a maximum and begin to decrease when the rate of gas expansion exceeds the gas generation rate. The RLPG cycle can be designed to operate at nearly constant pressure. Such pressure control has been demonstrated experimentally.[14 17] The RLPG interior ballistic cycle following propellant burnout is identical to that of a solid propellant gun.

The similarity of the solid and liquid propellant gun processes following propellant burnout is significant in that it permits a direct comparison of the evolution of the muzzle flow regions of the two systems.

IV. COMPUTATIONAL PROCEDURE

The muzzle flash computational procedure requires the use of several models to simulate the various processes in the muzzle flow region. These computer models, along with the major physical assumptions inherent in them, are briefly described below:

(a) BLAKE[11] is a model used to compute equilibrium thermodynamic properties, including equilibrium combustion products, of energetic materials.

(b) RLPTC[18] is a model used to compute the interior ballistic trajectory of a regenerative liquid propellant gun. This code uses the conservation equations for mass, momemtum and energy to model the physical processes occurring in this gun. The combustion chamber and propellant reservoir are treated as lumped parameter regions, while the barrel is treated as a one dimensional region.

(c) IBHVG[9] is a thermodynamic model used to compute the interior ballistic trajectory of a solid propellant gun. The combustion chamber is treated as a lumped parameter region as in the RLPTC model. However, a closed form solution to the governing equations is used in the barrel region.

(d) MEFF[6] is the model used to compute the flow field of the combustion gases at the gun muzzle after ejection of the projectile. This code models the blow-down process in the gun and the processes occuring in the expansion region ahead of the muzzle. The assumptions used have been described earlier.

(e) LAPP[13] is the model used to compute the gas composition, velocity, and pressure in the turbulent afterburning region by numerically integrating the conservation equations for mass, momemtum, and energy and the chemical kinetic equations. The main assumption used in this model is steady flow of gas from the end of the expansion region out to the interface between the blast wave and the ambient air.

(f) MTOB and CONCEN[12] are codes used to rearrange data for input to the BLAKE, and LAPP codes.

The procedure used to obtain muzzle flash predictions for a particular gun/propellant system has been outlined by Keller[12] and is illustrated in Figure 4. One first enters the propellant composition into the BLAKE code and from it obtains the thermodynamic properties of the propellant needed as input to the gun interior ballistic codes. Besides the output from the BLAKE code, additional input to the interior ballistic model consists of gun and projectile characteristics such as weight and dimensions, and additional propellant characteristics such as weight, shape and combustion characteristics. The output of the interior ballistic code needed by the MEFF code is the average gas temperature at muzzle exit, projectile velocity and mass, propellant mass, bore volume, propellant specific heat ratio, molecular weight, and covolume. The MEFF code then uses a simple gun bore evacuation model developed by Corner[10] to compute the flow of gas out of the gun. The data are then used to compute the flow field in the expansion region of the muzzle blast.

The output of the MEFF code is stored in a file, which serves as input to a data rearrangement code MTOB. The MTOB code was written to prepare data for thermodynamic calculations at several different locations in the muzzle exit flow field. The output of MTOB is subsquently be used by the BLAKE, CONCEN, and LAPP codes.

The BLAKE code is provided with output data from the MEFF code and propellant composition data as rearranged by the MTOB code, to compute gas compositions at the normal and reflected shocks. The BLAKE outputtogether with the MTOB output, is used as input to the CONCEN code. The CONCEN code computes the gas concentration at the interface between the expansion region and the turbulent afterburning region. The output of the CONCEN code is a list of the 17 gaseous species that the LAPP code will consider, and the mole fraction of each, in the exact order that LAPP expects to find them.

The LAPP code, using the CONCEN and MTOB output, then computes the gas composition and temperature throughout the turbulent afterburning region. Currently, 42 reaction equations are used in the model to compute the gas composition at various axial and radial locations in this region. Examination of this data and/or plots of gas temperature versus axial location provides the user of these codes with information regarding the probability of a muzzle flash.

Keller[12] has set up a procedure on the CYBER 7600 to automate the use of the MEFF, MTOB, CONCEN, BLAKE, and LAPP codes so that the occasional user can take the output from any interior ballistic code and readily determine the likelyhood of muzzle flash.

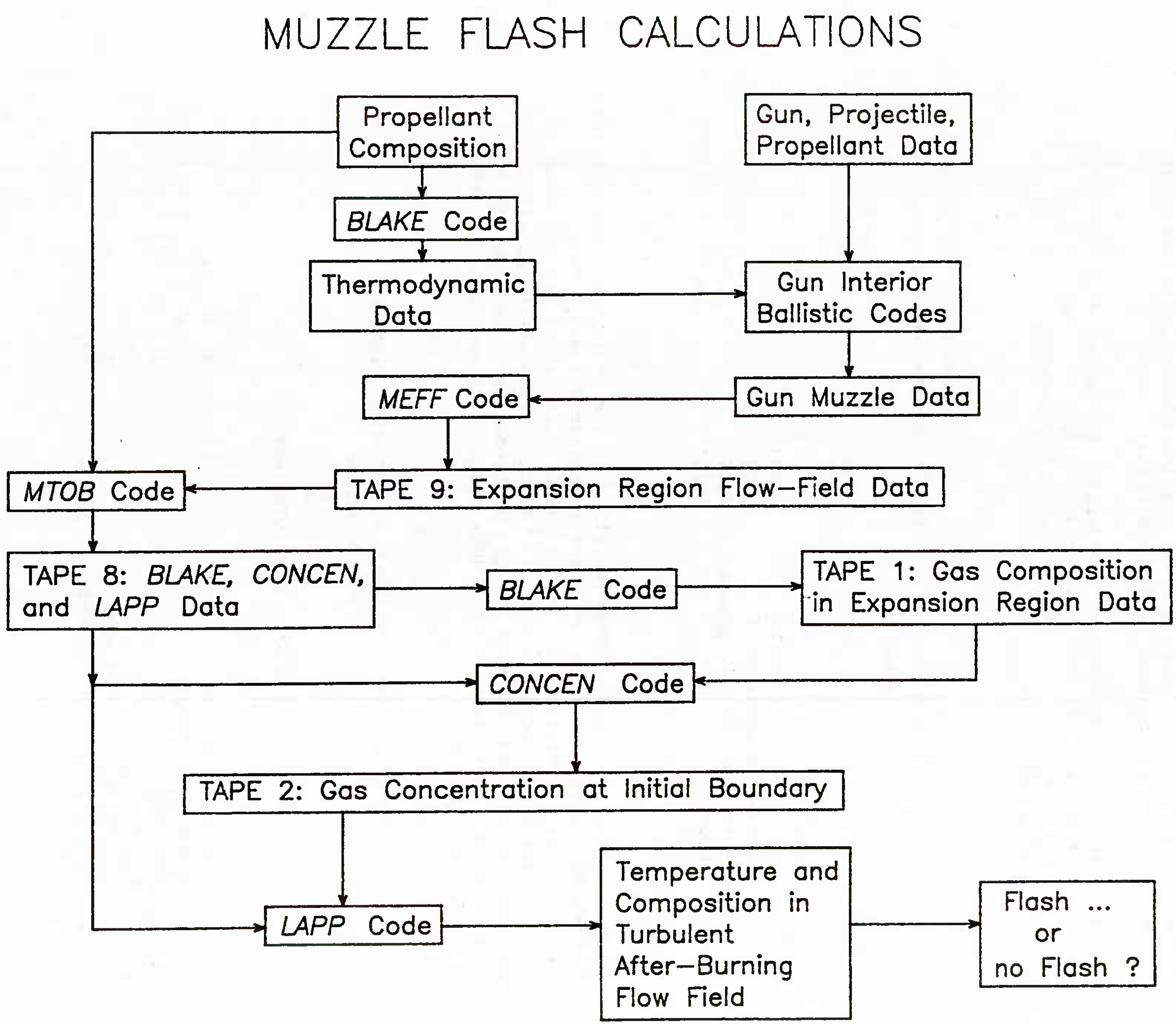

Figure 4. Muzzle Flash Computation Models

V. RESULTS

The computational procedure for predicting muzzle flash has been outlined in the previous section. The results of the individual computations are briefly sumarized summarized below.

The equilibrium thermodynamic properties of the two propellants used in this study, M30A1 and LGP 1845, were computed from the compositions listed in Table 1 and 2 for a loading density of 0.2 g/cc using the BLAKE code. These properties are listed in Table 3.

TABLE 3. Propellant Equilibrium Thermodynamic Properties

	M30A1	LGP 1845
Impetus (J/g)	1065.3	972.6
Specific Heat Ratio	1.241	1.215
Flame Temperature (K)	3003	2695
Molecular Weight (g/mole)	23.43	23.04
Covolume (cc/g)	1.041	0.609

The interior ballistic characteristics of the solid and a hypothetical regenerative liquid propellant guns are listed in Table 4. The characteristics associated with the projectile and barrel are the same for both solid and liquid propellant gun. The combustion of the liquid propellant has been adjusted to provide performance, maximum pressure and muzzle velocity, equivalent to that obtained in a 155-mm howitzer with an M203 propelling charge.

TABLE 4. Interior Ballistic Characteristics of 155-mm Howitzer

COMMON CHARACTERISTICS

Projectile Weight:	46.36	kg
Projectile Travel:	5.08	m
Bore Area:	192.44	cm^2
Muzzle Velocity:	808.	m/s
Maximum Chamber Pressure:	329.	MPa
Chamber Volume at Projectile Ejection:	19,664.	cm^3

Table 4. Interior Ballistic Characteristics of 155-mm Howitzer (Con't)

INDIVIDUAL CHARACTERISTICS

	SP GUN	RLP GUN
Initial Chamber Volume (cm^3):	19,664.	10,978.
Initial Liquid Propellant Volume (cm^3):	-	8,687.
Propellant Weight (kg):	12.23*	12.70
Propellant Density (g/cm^3):	1.582	1.462
Propellant-Projectile Weight Ratio (C/M):	0.264	0.274
Piston Weight (kg):	-	54.43
Piston Area, Chamber Side (cm^2):	-	547.
Piston Area, LP Side (cm^2):	-	401.

* Includes igniter components

The projectile base pressure vs projectile travel curves resulting from the interior ballistic trajectory simulations of both the solid propellant gun and the regenerative liquid propellant gun are illustrated in Figure 5. From the interior ballistic calculations, we obtain the gas pressures and temperatures at the muzzle given in Table 5. These muzzle conditions are used as inputs to BLAKE, from which the equilibrium gas compostion is determined.

TABLE 5. Muzzle Conditions at Projectile Exit for the Solid and Regenerative Liquid Propellant Guns

	SP GUN	RLP GUN
Muzzle Pressure (MPa)	70.36	73.92
Muzzle Temperature (K)	1828.	1915.

GAS COMPOSITION AT MUZZLE

Species	Concentrations (Mole Percent)		
	M30A1	LGP 1845	NS HAN LP**
N_2	27.65	17.41	16.47
CO_2	9.35	13.04	9.03
H_2O	22.42	69.46	58.66
H_2	14.96	0.03	9.42
CO	25.11	0.02	6.39
Others*	0.51	0.04	0.03

* Minor molecular species such as KOH, NH_3, O_2, etc.

** Artificially non-stoichiometric HAN liquid propellant formulation.

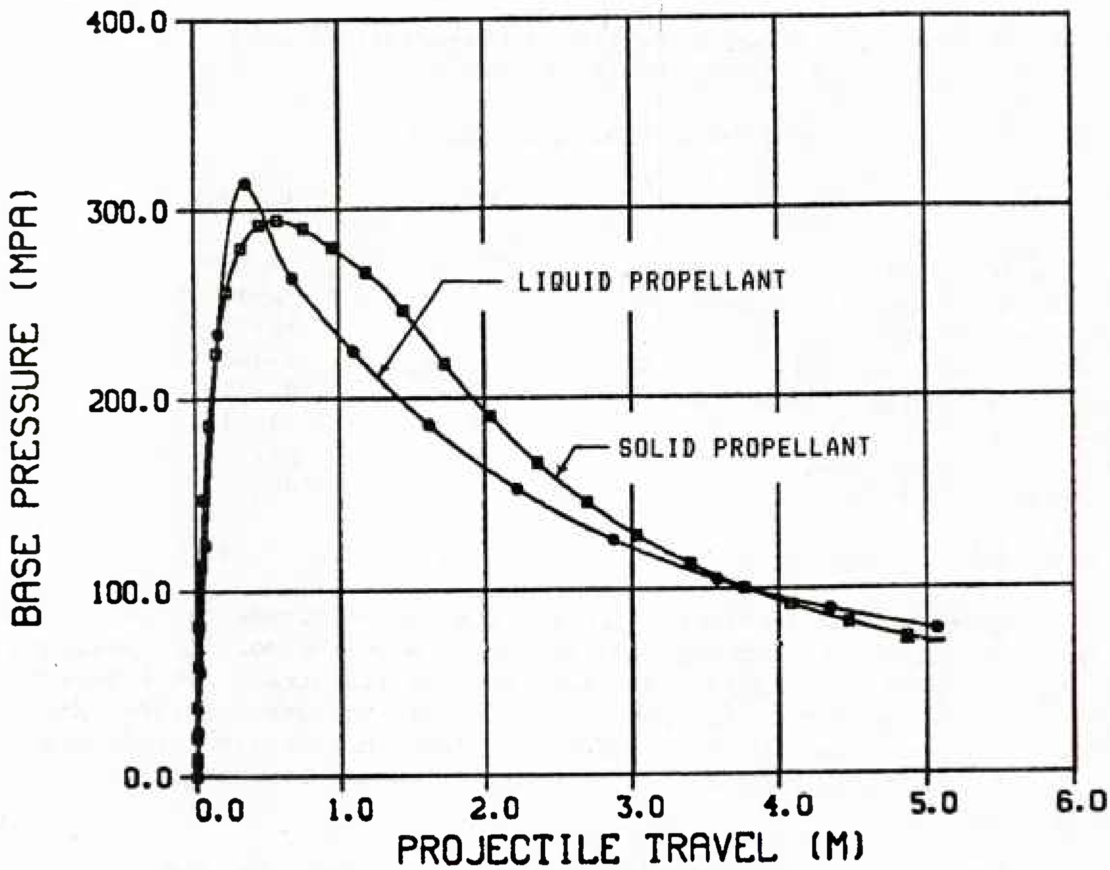

Figure 5. Base Pressure vs Projectile Travel for 155-mm Solid and Regenerative Liquid Propellant Guns.

The solid propellant combustion gases are extremely fuel-rich at muzzle conditions as would be expected. CO and H_2 represent 40% the combustion products in the case of the M30A1 propellant. However, the muzzle exhaust of the stoichiometric LGP 1845 contains less than 0.1% of gases other than N_2, CO_2 and H_2O. During the present study, an error was made in the specification of the composition of LGP 1845, resulting in a hypothetical, fuel rich HAN-based propellant. The error was easily detected when the BLAKE output indicated a non-stoichiometric propellant had been used. The calculations made using the hypothetical propellant have been retained to provide an intermediate case, with approximately 16% non-reacted material in the exhaust gases, for comparison.

The gas stream temperature, pressure, velocity, and composition at the entrance to the turbulent afterburning region is given in Table 4. As previuosly noted, the propellant gases expand isentropically from the muzzle to the reflected shock. With the assumption of frozen chemistry in the expansion region, the species mole fractions in the reflected shock region are equal to their values at the muzzle, Table 5. Using the pressure and temperature of the normal shock, BLAKE is again used to calculate the species mole fractions at this location. The species mole fractions at the reflected and normal shock locations are then averaged to obtain the species mole fractions at the entrance to the turbulent afterburning region which are presented in Table 6.

TABLE 6. Conditions at Entrance to Turbulent Afterburning Region for the Solid and Regenerative Liquid Propellant Guns

	SP GUN	RLP GUN
Pressure (MPa)	1.01	1.01
Temperature (K)	988.	1053.
Velocity (m/s)	1933.	2058.

GAS COMPOSITION AT ENTRANCE

Species	Concentrations (Mole Percent)		
	M30A1	LGP 1845	NS HAN LP**
N_2	27.70	17.40	16.48
CO_2	9.34	12.97	9.02
H_2O	22.49	69.33	58.67
H_2	14.99	0.09	9.41
CO	25.20	0.08	6.40
Others*	0.28	0.03	0.02

* Minor molecular species such as KOH, NH3, O2, etc.
** Non- stoichmetric HAN liquid propellant formulation.

The flow of muzzle gas from the gun muzzle through the expansion region to the interface between the expansion region and the turbulent afterburning region results in a reduction of pressure and temperature, and an increase in gas velocity. There is also a minor change in gas composition, consistent with the assumption of frozen chemistry for approximately 90% of the flow passing through the reflected shock and equilibrium chemistry for the remaining 10% which passes through the normal shock.

In the turbulent afterburning region the combustion gases mix with air resulting in further reaction and a rise in gas temperature. A plot of the centerline gas temperature in the exhaust plume versus distance from the initial plane separating the turbulent afterburning region from the expansion region is illustrated in Figure 6 for the three propellants. The M30A1 solid propellant case shows the steepest rise in temperature. The temperature rise begins about 14 m from the initial plane and reaches a maximum value of 2175 K, an increase of 1187 K, about 47 m from the initial plane. This increase in temperature results from the combustion of the large amount of hydrogen and carbon monoxide (about 40%) present. The increase in temperature in the case of LGP 1845 is only 94 K, consistent with the very small amount of unreacted material in the muzzle exhaust. The predicted increase in temperature for the non-stoichmetric, HAN-based LP is 633 K, indicative of substantial energy release due to combustion.

VI. DISCUSSION

The results as illustrated in Figure 6 indicate that the solid propellant gun using M30A1 propellant without flash suppressant will exhibit a strong secondary flash and blast wave due to the burning of the fuel-rich propellant gases in the turbulent afterburning region. This is indicated by the 1187 K rise in gas temperature over a distance of approximately 30 m. Secondary flash has indeed been observed in firings of the 155-mm howitzer using the projectile/charge combination considered in this study.

In the case of the stoichiometric HAN-based monopropellant, LGP 1845, only a small rise in temperature in the turbulent afterburning region is predicted. This result is consistent with the very small amount of unreacted material present in the muzzle exhaust gases. Based on the small rise in temperature predicted in this case, it is unlikely that any secondary flash would be obtained in actual gun firings.

The results obtained in the case of the hypothetical non-stoichiometric HAN-based LP are interesting and informative in that they indicate a temperature rise in the turbulent afterburning region which falls between the two previous cases. The muzzle exhaust products of the non-stoichiometric, HAN-based LP contain about 15% unreacted products, versus about 40% for M30A1 and less than 0.1% for LGP 1845. The results in Figure 7 indicate that in all three cases the combustible material present in the afterburning region reacted, releasing the available energy. Thus the gun muzzle conditions, i.e. pressure and temperature, favor secondary flash in all cases. The controlling factor is, therefore, the amount of combustible material present in the muzzle exhaust.

It should be noted that the muzzle temperature in the RLPG calculations is 87 K higher than the calculated muzzle temperature in the solid propellant case, despite the 308 K higher isochoric flame temperature of the solid propellant. This result would appear contrary to our current concepts regarding gun interior ballistics. This apparent paradox is being investigated, but no explanations are available at this time. However, there are two facts worth noting. First, the interior ballistic calculations used in the solid propellant and RLPG cases are quite different. In the solid propellant case, an approximate analytical solution is used for the barrel flow, while a one dimensional hydrodynamic model is used in the RLPG simulation. Secondly, the higher muzzle temperature in the RLPG case favors muzzle flash. Therefore, the predicted temperature rise in the LGP 1845 calculations represents a "worst case" situation, and the conclusion that no muzzle flash is expected for the stoichiometric propellant is not affected by the muzzle temperature paradox.

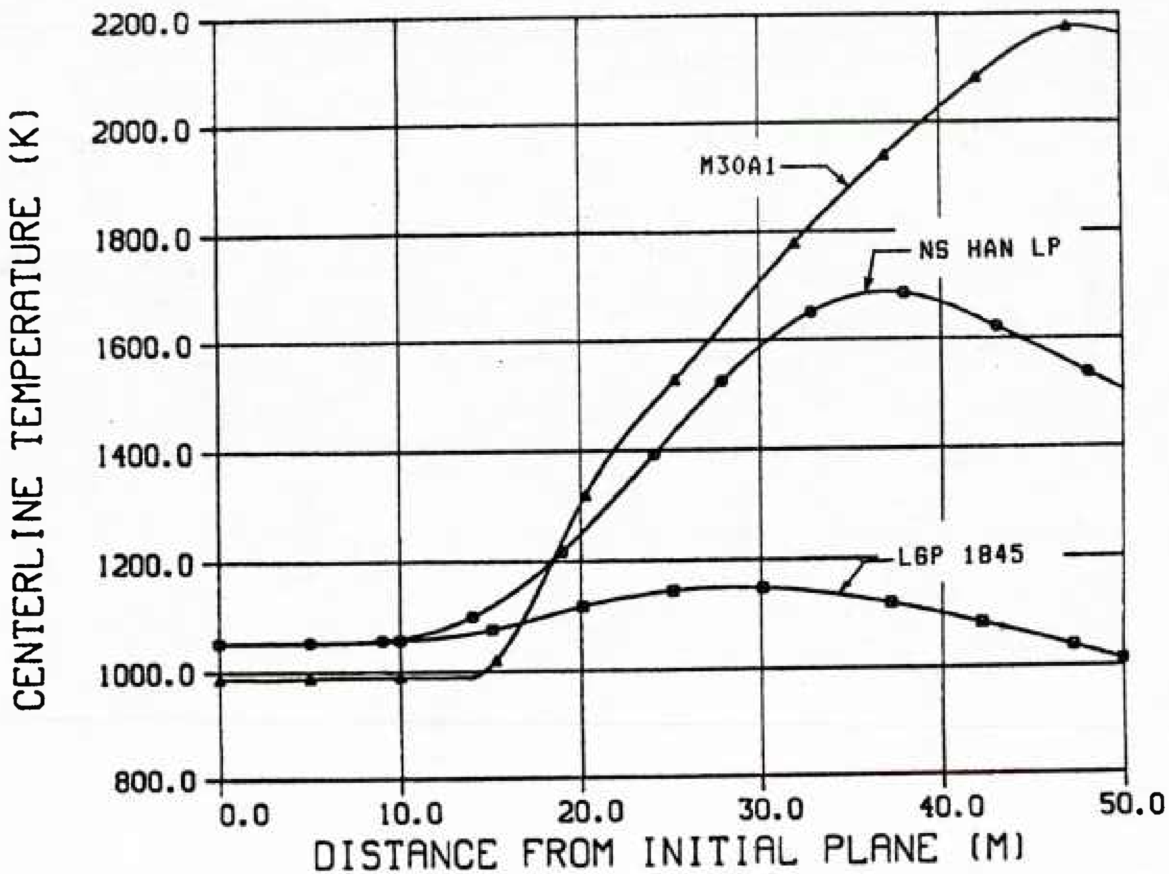

Figure 6. Center Line Temperatures in Turbulent Afterburning Region for Solid and Liquid Propellants.

Future efforts in this area will focus on the resolution of the muzzle temperature paradox, and a determination of the sensitivity of predicted secondary flash to variations of propellant formulation.

REFERENCES

1. Carfagno, S.P., Handbook on Gun Flash, The Franklin Institute, Contract No. DA-36-034-501-ORD-78RD, Nov., 1961 (AD327051).

2. May, I.W. and Einstein, S.I., "Prediction of Gun Muzzle Flash," U.S. Army Ballistic Research Laboratory Report ARBRL-TR-02229, March 1980.

3. Schmidt, E.M., "Secondary Combustion in Gun Exhaust Flows," U.S. Army Ballistic Research Laboratory Report ARBRL-TR-02373, October 1981.

4. Klingenberg, G., "Analysis of Gun Muzzle Flash Phenomena," Proc. 4th International Symposium on Ballistics, Monterey, Calif., 17-10 Oct 1978.

5. Schmidt, E.M. and Shear, D.D., "Optical Measurements of Muzzle Blast," AIAA Journal, Vol. 13, No. 8, august 1975.

6. Yousefian, V., "Muzzle Flash Onset," U.S. Army Ballistic Research Laboatory Report ARBRL-CR-00477, February 1982.

7. Heimerl, J.M., "Muzzle Flash and Alkali Salt Inhibition From An Elementary Kinetic Point Of View," U.S. Army Ballistic Research Laboratory Report ARBRL-TR-02479, March 1983.

8. Yousefian, V., May, I.W., and Heimerl, J.M., "Modeling the Occurrence of Muzzle Flash in Guns," 17th JANNAF Combustion Meeting, CPIA Publication 329, November 1980.

9. Anderson, R.D. and Fickie, K.D., "IBHVG2 - A User's Guide," Ballistic Research Laboratory Report in preparation.

10. Corner, J., Theory of the Interior Ballistics of Guns, pp. 370-374, John Wiley & Sons, Inc., New York, 1950.

11. Freedman, E., "BLAKE-A Thermodynamics Code Based on Tiger: Users' Guide and Manual," Technical Report ARBRL-TR-02411, July 1982.

12. Keller, G., "A MEFF User's Guide," ARBRL-MR-03362, July 1984.

13. Mikatarian, R.R., Kau, C.J., and Pergament, H.S., "A Fast Computer Program for Nonequilibrium Rocket Plume Prediction," Air Force Rocket Propulsion Laboratory, Report No. AFRPL-TR-72-94, August 1972.

14. Krier, H. and Summerfield, M., ed. Interior Ballistics of Guns, Progress in Astronautics and Aeronautics, Vol. 66, AIAA, New York, 1979.

15. Morrison, W.F., Knapton, J.D., and Klingenberg, G., "Liquid Propellants For Gun Application," Proceedings of the Seventh International Symposium on Ballistics, 1983.

16. Mandzy, J., Magoon, I., Morrison, W.F., and Knapton, J.D., "Preliminary Report on Test Firings of a 105-mm Regenerative Fixture," Proceedings of the Twentieth JANNAF Combustion Meeting, 1983.

17. Hassenbein, R.G., "Regenerative Liquid Propellant Gun Technology," ARLCB-TR-81026, June 1981.

18. Gough, P.S., "A Model of the Interior Ballistics of Hybrid Liquid-Propellant Guns," Paul Gough Associates, PGA-TR-83-4, September 1983.

DISTRIBUTION LIST

No. of Copies	Organization
12	Commander Defense Technical Info Center ATTN: DTIC-DDA Cameron Station Alexandria, VA 22304-6145
1	Director Defense Advanced Research Projects Agency ATTN: H. Fair 1400 Wilson Boulevard Arlington, VA 22209
1	HQDA DAMA-ART-M Washington, DC 20310
1	Commander US Army Materiel Command ATTN: AMCDRA-ST 5001 Eisenhower Avenue Alexandria, VA 22333-0001
13	Commander Armament R&D Center US Army AMCCOM ATTN: SMCAR-TSS SMCAR-TDC SMCAR-SCA, B. Brodman R. Yalamanchili SMCAR-AEE-B, D. Downs A. Beardell SMCAR-LCE, N. Slagg SMCAR-LCS, W. Quine A. Bracuti J. Lannon SMCAR-FSS-A, R. Price L. Frauen SMCAR-FSA-S, H. Liberman Picatinny Arsenal, NJ 07806-5000
3	Director Benet Weapons Laboratory Armament R&D Center US Army AMCCOM ATTN: SMCAR-LCB-TL E. Conroy A. Graham Watervliet, NY 12189
1	Commander US Army Armament, Munitions and Chemical Command ATTN: SMCAR-ESP-L Rock Island, IL 61299-7300
1	Commander US Army Aviation Research and Development Command ATTN: AMSAV-E 4300 Goodfellow Blvd. St. Louis, MO 63120
1	Commander Materials Technology Lab US Army Laboratory Cmd ATTN: SLCMT-MCM-SB M. Levy Watertown, MA 02172-0001
1	Director US Army Air Mobility Rsch. and Development Lab. Ames Research Center Moffett Field, CA 94035
1	Commander US Army Communications Electronics Command ATTN: AMSEL-ED Fort Monmouth, NJ 07703
1	Commander ERADCOM Technical Library ATTN: STET-L Ft. Monmouth, NJ 07703-5301

DISTRIBUTION LIST

No. of Copies	Organization
1	Commander US Army Harry Diamond Labs ATTN: DELHD-TA-L 2800 Powder Mill Rd Adelphi, MD 20783
1	Commander US Army Missile Command Rsch, Dev, & Engr Ctr ATTN: AMSMI-RD Redstone Arsenal, AL 35898
1	Commander US Army Missile & Space Intelligence Center ATTN: AIAMS-YDL Redstone Arsenal, AL 35898-5500
1	Commander US Army Belvoir R&D Ctr ATTN: STRBE-WC Tech Library (Vault) B-315 Fort Belvoir, VA 22060-5606
1	Commander US Army Tank Automotive Cmd ATTN: AMSTA-TSL Warren, MI 48397-5000
1	Commander US Army Research Office ATTN: Tech Library P.O. Box 12211 Research Triangle Park,NC 27709-2211
1	Director US Army TRADOC Systems Analysis Activity ATTN: ATAA-SL White Sands Missile Range NM 88002
1	Commandant US Army Infantry School ATTN: ATSH-CD-CSO-OR Fort Benning, GA 31905

No. of Copies	Organization
1	Commander Armament Rsch & Dev Ctr US Army Armament, Munitions and Chemical Command ATTN: SMCAR-CCS-C, T Hung Picatinny Arsenal, NJ 07806-5000
1	Commandant US Army Field Artillery School ATTN: ATSF-CMW Ft Sill, OK 73503
1	Commandant US Army Armor Center ATTN: ATSB-CD-MLD Ft Knox, KY 40121
1	Commander US Army Development and Employment Agency ATTN: MODE-TED-SAB Fort Lewis, WA 98433
1	Commander Naval Surface Weapons Center ATTN: D.A. Wilson, Code G31 Dahlgren, VA 22448-5000
1	Commander Naval Surface Weapons Center ATTN: Code G33, J. East Dahlgren, VA 22448-5000
2	Commander US Naval Surface Weapons Ctr. ATTN: O. Dengel K. Thorsted Silver Spring, MD 20902-5000
1	Commander Naval Weapons Center China Lake, CA 93555-6001
1	Commander Naval Ordnance Station ATTN: C. Dale Code 5251 Indian Head, MD 20640

DISTRIBUTION LIST

No. of Copies	Organization
1	Superintendent Naval Postgraduate School Dept of Mechanical Eng. ATTN: Code 1424, Library Monterey, CA 93943
1	AFWL/SUL Kirtland AFB, NW 87117
1	Air Force Armament Lab ATTN: AFATL/DLODL Eglin, AFB, FL 32542-5000
1	AFOSR/NA (L. Caveny) Bldg. 410 Bolling AFB, DC 20332
1	Commandant USAFAS ATTN: ATSF-TSM-CN Ft Sill, OK 73503-5600
1	US Bureau of Mines ATTN: R.A. Watson 4800 Forbes Street Pittsburgh, PA 15213
1	Director Jet Propulsion Lab ATTN: Tech Libr 4800 Oak Grove Drive Pasadena, CA 91109
2	Director National Aeronautics and Space Administration ATTN: MS-603, Tech Lib MS-86, Dr. Povinelli 21000 Brookpark Road Lewis Research Center Cleveland, OH 44135
1	Director National Aeronautics and Space Administration Manned Spacecraft Center Houston, TX 77058

No. of Copies	Organization
10	Central Intelligence Agency Office of Central Reference Dissemination Branch Room GE-47 HQS Washington, DC 20502
1	Central Intelligence Agency ATTN: Joseph E. Backofen HQ Room 5F22 Washington, DC 20505
4	Bell Aerospace Textron ATTN: F. Boorady K. Berman A.J. Friona J. Rockenfeller Post Office Box One Buffalo, NY 14240
1	Calspan Corporation ATTN: Tech Library P.O. Box 400 Buffalo, NY 14225
7	General Electric Ord. Sys Dpt ATTN: J. Mandzy, OP43-220 R.E. Mayer H. West M. Bulman R. Pate I. Magoon J. Scudiere 100 Plastics Avenue Pittsfield, MA 01201-3698
1	General Electric Company Armanent Systems Department ATTN: D. Maher Burlington, VT 05401
1	IITRI ATTN: Library 10 W. 35th St. Chicago, IL 60616
1	Olin Chemicals Research ATTN: David Gavin P.O. Box 586 Chesire, CT 06410-0586

DISTRIBUTION LIST

No. of Copies	Organization
2	Olin Corporation ATTN: Victor A. Corso Dr. Ronald L. Dotson P.O. Box 30-9644 New Haven, CT 06536
1	Paul Gough Associates ATTN: Paul Gough PO Box 1614 Portsmouth, NH 03801
1	Safety Consulting Engr ATTN: Mr. C. James Dahn 5240 Pearl St. Rosemont, IL 60018
1	Science Applications, Inc. ATTN: R. Edelman 23146 Cumorah Crest Woodland Hills, CA 91364
1	Sunstrand Aviation Operations ATTN: Dr. Owen Briles P.O. Box 7002 Rockford, IL 61125
1	Veritay Technology, Inc. ATTN: E. B. Fisher 4845 Millersport Highway, P.O. Box 305 East Amherst, NY 14051-0305
1	Director Applied Physics Laboratory The Johns Hopkins Univ. Johns Hopkins Road Laurel, Md 20707
2	Director Chemical Propulsion Info Agency The Johns Hopkins Univ. ATTN: T. Christian Tech Lib Johns Hopkins Road Laurel, MD 20707

No. of Copies	Organization
2	University of Delaware Department of Chemistry ATTN: Mr. James Cronin Professor Thomas Brill Newark, DE 19711
1	U. of ILLinois at Chicago ATTN: Professor Sohail Murad Dept of Chemical Eng Box 4348 Chicago, IL 60680
1	U. of Maryland at College Park ATTN: Professor Franz Kasler Department of Chemistry College Park, MD 20742
1	U. of Missouri at Columbia ATTN: Professor R. Thompson Department of Chemistry Columbia, MO 65211
1	U. of Michigan ATTN: Prof. Gerard M. Faeth Department of Aerospace Engineering Ann Arbor, MI 48109-3796
1	U. of Missouri at Columbia ATTN: Professor F. K. Ross Research Reactor Columbia, MO 65211
1	U. of Missouri at Kansas City Department of Physics ATTN: Prof. R.D. Murphy 1110 East 48th Street Kansas City, MO 64110-2499
1	Pennsylvania State University Dept. of Mechnical Eng ATTN: K. Kuo University Park, PA 16802

DISTRIBUTION LIST

No. of Copies	Organization
2	Princeton Combustion Rsch Laboratories, Inc. ATTN: N.A. Messina M. Summerfield 475 US Highway One North Monmouth Junction, NJ 08852
1	University of Arkansas Department of Chemical Engineering ATTN: J. Havens 227 Engineering Building Fayetteville, AR 72701

Aberdeen Proving Ground

Dir, USAMSAA
ATTN: AMXSY-D
AMXSY-MP, H. Cohen

Cdr, USATECOM
ATTN: AMSTE-TO-F

CDR, CRDEC, AMCCOM
ATTN: SMCCR-RSP-A
SMCCR-MU
SMCCR-SPS-IL

USER EVALUATION SHEET/CHANGE OF ADDRESS

This Laboratory undertakes a continuing effort to improve the quality of the reports it publishes. Your comments/answers to the items/questions below will aid us in our efforts.

1. BRL Report Number ______________________ Date of Report __________

2. Date Report Received ______________________________________

3. Does this report satisfy a need? (Comment on purpose, related project, or other area of interest for which the report will be used.) ______________

4. How specifically, is the report being used? (Information source, design data, procedure, source of ideas, etc.) ______________

5. Has the information in this report led to any quantitative savings as far as man-hours or dollars saved, operating costs avoided or efficiencies achieved, etc? If so, please elaborate. ______________

6. General Comments. What do you think should be changed to improve future reports? (Indicate changes to organization, technical content, format, etc.)

CURRENT ADDRESS

____
Name

____
Organization

____
Address

____
City, State, Zip

7. If indicating a Change of Address or Address Correction, please provide the New or Correct Address in Block 6 above and the Old or Incorrect address below.

OLD ADDRESS

____
Name

____
Organization

____
Address

____
City, State, Zip

(Remove this sheet, fold as indicated, staple or tape closed, and mail.)

— — — — — — — — — — FOLD HERE — — — — — — — — — — —

Director
US Army Ballistic Research Laboratory
ATTN: DRXBR-OD-ST
Aberdeen Proving Ground, MD 21005-5066

NO POSTAGE NECESSARY IF MAILED IN THE UNITED STATES

OFFICIAL BUSINESS
PENALTY FOR PRIVATE USE, $300

BUSINESS REPLY MAIL
FIRST CLASS PERMIT NO 12062 WASHINGTON, DC

POSTAGE WILL BE PAID BY DEPARTMENT OF THE ARMY

Director
US Army Ballistic Research Laboratory
ATTN: DRXBR-OD-ST
Aberdeen Proving Ground, MD 21005-9989

— — — — — — — — — — FOLD HERE — — — — — — — — — — —